Bioconjugate Chemistry

Article

pubs.acs.org/bc

Investigation into Temperature-Induced Aggregation of an Antibody Drug Conjugate

Nia S. Beckley,*[,†] Kathlyn P. Lazzareschi,[‡] Hung-Wei Chih,[§] Vikas K. Sharma,[†] and Heather L. Flores*[,†]

[†]Early Stage Pharmaceutical Development, [‡]Purification Development, and [§]Late Stage Pharmaceutical and Process Development, Genentech, Inc., 1 DNA Way, South San Francisco, California 94080, United States

Supporting Information

ABSTRACT: Conjugation of an antibody to a drug can produce heterogeneous species that may have different physical stabilities and safety profiles. We explored the effect of thermal stress on the physical stability, specifically aggregation, of an antibody drug conjugate (ADC), ADC 1, wherein the antibody was linked to the val-cit-Monomethyl Auristatin E (vc-MMAE) linker drug through the reduction of interchain disulfides. We also explored the effects of conjugation on the secondary and tertiary structures of ADC 1. Circular dichroism, intrinsic tryptophan fluorescence, and differential scanning calorimetry showed that for species with high drug loading, conjugation does not measurably alter the secondary structure, but it does render the CH_2 domain less stable to thermal stress such that ADC 1 rapidly forms high molecular weight species (HMWS) at 40 °C. Characterization of the HMWS using chromatographic and electrophoretic methods showed that it is an irreversible, noncovalent, and structurally altered form of ADC 1 primarily composed of molecules with six or eight drugs. Furthermore, the variable domain of the antibody may contribute to the extent of aggregation, since eight ADCs with over 90% sequence homology exhibited monthly rates of HMWS formation that differ by up to a factor of 2.

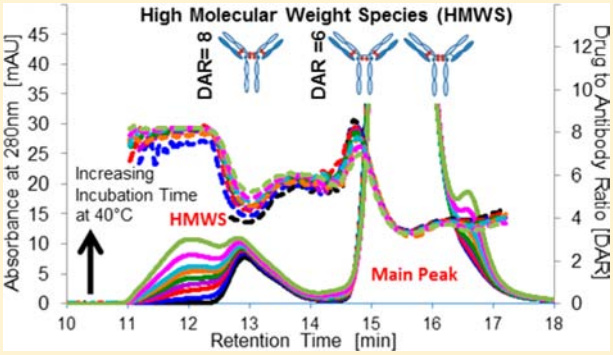

INTRODUCTION

Antibody drug conjugates (ADCs) are a class of antibody-based compounds whose therapeutic efficacy relies on the specificity of an antibody and the potency of a chemotherapeutic drug that is linked to the antibody via chemical conjugation.[1−4] The antibody first binds to the target antigen and becomes internalized by the target cancer cell.[2] Then the chemotherapeutic drug, typically after being released from the antibody via either acid hydrolysis or lysosomal enzymes, kills the cell by targeting an essential cellular component such as microtubules or DNA.[5−10] Thus, with the addition of the drug, the ADC is better poised to ensure that the target cells are destroyed.[8−11] Currently, several ADCs are in the advanced stages of clinical trials, with two recently approved by the FDA.[6,12]

The chemotherapeutic drugs used in ADCs include highly effective chemotoxins, such as maytansinoids and auristatins.[5] These chemotherapeutic agents are chemically linked to a noncleavable or cleavable linker, which is then further chemically linked to the antibody via specific reaction chemistries that produce a conjugated product; some linkers are designed to conjugate to lysine residues, while others are tailored for thiol residues.[5] Such conjugation, however, often leads to a distribution of drug load on the antibody, as conjugating an exact number of drugs to all antibodies in a system is chemically challenging. For the thiol-based chemistry, where the conjugation process relies on the reduction of interchain disulfide bonds, the "average" drug-to-antibody ratio, or DAR, is controlled largely by the extent to which the bulk antibody interchain disulfide bonds are reduced during the conjugation process.[11] Ultimately, a conjugation process that relies on the nonspecific reduction of these bonds typically produces a distribution of antibodies with DARs ranging from 0 to 8, and also a distribution of positional isomers for a given DAR (Figure 1).[5,13]

With the emergence of this new class of therapeutic agents comes a new wave of efforts to understand the effect of drug loading on the therapeutic potential[11] and stability of monoclonal antibodies. Since the interchain disulfide bonds are known to stabilize the quaternary structure of a typical antibody, disrupting these bonds with hydrophobic drugs could affect the overall physical stability of the molecule.[14] Therefore, it is reasonable to ask whether ADC DAR subspecies and positional isomers produced by the conjugation process have different stabilities, particularly physical stabilities. Understanding how this chemical modification affects the stability of the antibody will improve the early molecular assessment of ADC candidates with the same target and reduce the effort that pharmaceutical scientists exert trying to mitigate ADC-specific physical instabilities.

Received: April 12, 2013
Revised: September 10, 2013
Published: September 12, 2013

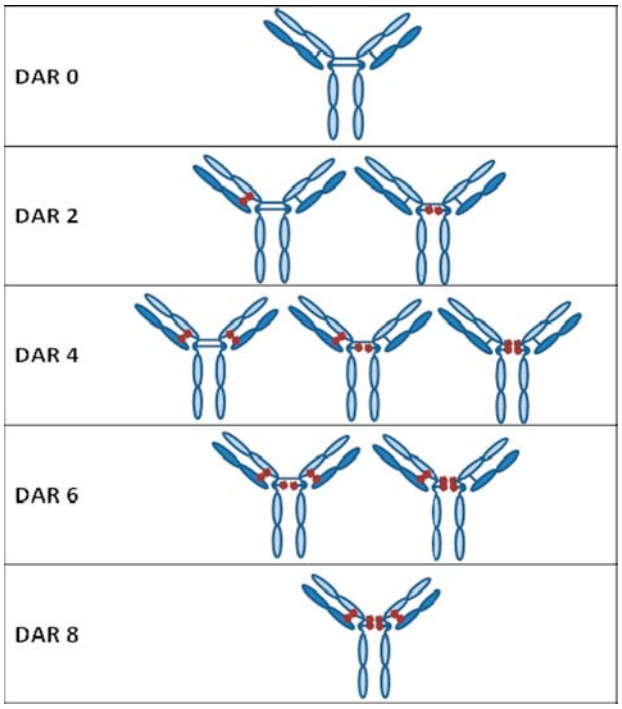

Figure 1. DAR isoforms resulting from conjugation of interchain disulfides in ADCs.

In this study, we explore the effects of conjugation and DAR on the physical stability, i.e., aggregation, of an ADC (hereon referred to as ADC 1) with an average DAR of 3.5 that was conjugated via the reduction of interchain disulfide bonds. A stress temperature of 40 °C was used to amplify differences in the stabilities of ADC subspecies, and ultimately to define the biophysical properties of the aggregates and determine how drug loading affects the formation of these species. We also characterized the secondary and tertiary structure of the ADC and the aggregate to understand the conformational consequences of conjugation and aggregation. Finally, we present data on the physical stability of several ADCs to explore the generality of this behavior.

MATERIALS AND METHODS

Materials. ADCs 1 through 8 are IgG1 recombinant humanized monoclonal antibody–drug conjugates manufactured by Genentech in South San Francisco, California, United States. Research lots of ADC 1 were conjugated to have average DARs of 2, 3.5, and 6. All ADC 1 lots were produced from the same starting lot of unconjugated antibody. In order to produce these three average DARs, predefined molar ratios of tris (2-carboxyethyl) phosphine were mixed with the antibody to reduce only a fraction of the interchain disulfide bonds. The partially reduced antibody was then combined with a predefined molar ratio of val-cit monomethyl auristatin E (vc-MMAE) in dimethylacetamide. Conjugation was achieved when the maleimide group of the linker drug reacted with free cysteines on the antibody. The unreacted maleimide residues of any unconjugated vc-MMAE were then quenched by the addition of a predefined molar ratio of *n*-acetyl cysteine. After conjugation, the lots were dialyzed overnight at 5 °C into a 20 mM buffer, adjusted to pH 5.5, and concentrated to 10 mg/mL. Drug load distributions of each lot were confirmed by hydrophobic interaction chromatography (Supporting Information (SI) Figure S1). Since the vc-MMAE moiety is very hydrophobic, peaks with later retention times correspond to antibody fractions with higher drug loads. ADC 1 lots were stored at −70 °C prior to being thermally stressed.

Neat solutions of ADC 1 stored in glass vials were placed at 40 °C (protected from light) in order to thermally stress them. This temperature is commonly used to screen for degradation (i.e., aggregation) in an antibody, and can provide information about changes that may occur at the drug product storage temperature of 5 °C over the long term. The concentration of all ADC 1 lots was determined by UV spectroscopy at 278 nm, using an absorbance of 1.39 for a 1 mg/mL solution in a 1 cm cell. All stressed stability samples were stored at −70 °C until analysis. All ADCs were in the same formulation, except for ADC 4 and ADC 8, which are formulated at 20 mM in different buffers at pH 6.5 and 6.0, respectively.

Hydrophobic Interaction Chromatography (HIC). An Agilent 1200 series HPLC with the TSK-Gel Butyl-NPR column (4.6 mm × 35 mm) was used to separate and quantify antibody degradation products of different DARs. Mobile phase A was composed of 1.5 M ammonium sulfate, 25 mM sodium phosphate pH 6.95, while mobile phase B consisted of 25% IPA in 25 mM sodium phosphate pH 6.95. Samples (10 μL of 10 mg/mL) of ADC 1 were injected neat onto the column at a flow rate of 0.8 mL/min, with a gradient of 0% to 100% mobile phase B from 0 to 12.0 min, followed by a column flush of 100% A from 12.1 to 18.0 min. Absorbance was detected at 280 nm, 248 nm, and 214 nm. Samples were stored at 5 °C during analysis.

Size Exclusion Chromatography (SEC) with Multi-Angle Light Scattering (MALS) and Fraction Collection. The Agilent 1200 series HPLC with the TSKGel G3000 SWXL column (7.8 × 300 mm, 5 μm) was used to separate antibody degradation products by size. The mobile phase was composed of 0.2 M potassium phosphate, 0.25 M potassium chloride, pH 6.95 with 7.5% IPA, which was added to improve the resolution of the low molecular weight species (LMWS). After thermal stress, 10 μL of 10 mg/mL ADC 1 was injected neat onto the column at a flow rate of 0.5 mL/min. Absorbance was detected at 280 nm, 248 nm, and 214 nm. When fraction collection was performed, isopropanol was not included in the mobile phase to avoid compromising the stability of collected fractions. Peaks were fraction collected by choosing elution times that corresponded to ±30% of the peak maximum retention time. Fraction collected pools for each peak were pooled, centrifugally concentrated to 10 mg/mL (main peak) or 1.5 mg/mL (HMWS), and buffer exchanged into either water (for reverse phase and SEC analysis) or 20 mM buffer at pH 5.5 (for all other analysis) using an Amicon 10 000 K centrifugal filter. Fraction-collected samples were reinjected onto the SEC column using mobile phase with and without alcohol to confirm that the proper peak was fraction-collected. The concentration and turbidity of all fraction-collected samples was obtained to determine if scattering should be considered during sample analysis. All samples were clear (nonturbid), and no visual particulates were observed. Samples were stored at 5 °C until further analysis. SEC-MALS was run using an Agilent 1100 HPLC with two inline TSK-Gel G3000 SWXL (7.8 × 300 mm, 5 μm) columns in an isocratic method with a 0.25 mL/min flow rate, using 0.2 M potassium phosphate, 0.25 M potassium chloride, pH 6.95 with 5% IPA as the mobile phase. The column compartment temperature was set to room temperature, the run time was 100 min, and 100 μL of 10

dx.doi.org/10.1021/bc400182x | *Bioconjugate Chem.* 2013, 24, 1674–1683

mg/mL ADC solution was injected onto the column. The MALS detection was performed using a multiangle light scattering detector with a 590 nm laser (Dawn Heleos, Wyatt Technology). Protein concentration was determined by absorbance at 280 nm or by refractive index at 590 nm (Optilab rex, Wyatt Technology). A refractive index increment (dn/dc) of 0.185 was used for protein. The average molecular weight was determined with a Debye plot using Wyatt ASTRA software (version 6.0.3).

DAR by UV. The average drug to antibody ratio (DAR) was calculated by UV analysis during the SEC or HIC run by using the absorbance of a protein and drug at 248 nm (drug absorbance maxima) and 280 nm (protein absorbance maxima) in the following equations described by Hamblett et al.[15]

$$A^{248}_{\text{Total}} = \varepsilon^{248}_{\text{Ab}} C_{\text{Ab}} + \varepsilon^{248}_{\text{Drug}} C_{\text{Drug}} \quad (1a)$$

$$A^{280}_{\text{Total}} = \varepsilon^{280}_{\text{Ab}} C_{\text{Ab}} + \varepsilon^{280}_{\text{Drug}} C_{\text{Drug}} \quad (1b)$$

$$\text{DAR} = \frac{\varepsilon^{248}_{\text{Ab}} - R\varepsilon^{280}_{\text{Ab}}}{R\varepsilon^{280}_{\text{Drug}} - \varepsilon^{248}_{\text{Drug}}} \quad (2)$$

where R is the ratio of total absorbance at 248 nm to that at 280 nm, C_{ab} is the concentration of the antibody, C_{drug} is the concentration of the drug, and ε is the extinction coefficient of the drug or antibody at a relevant wavelength in L/(gcm). These equations assume a path length of 1 cm. In order to use this equation, it was necessary to determine the extinction coefficient of the unconjugated antibody in the SEC and HIC chromatography environments at 248 nm, since these values are crucial to the accurate calculation of the drug to antibody ratio and can be largely influenced by the chemical environment at this wavelength. The unconjugated ADC 1 precursor was run on both assays, and the absorbance of the peak maximum was used to determine the extinction coefficient for which a DAR of 0 would result. The values of the extinction coefficients of the antibody and drug in the SEC system were as follows: $\varepsilon_{\text{Ab},280} = 2.09 \times 10^5$ L/(mol cm), $\varepsilon_{\text{Ab},248} = 8.94 \times 10^4$ L/(mol cm), $\varepsilon_{\text{Drug},280} = 1.50 \times 10^3$ L/(mol cm), and $\varepsilon_{\text{Drug},248} = 1.59 \times 10^4$ L/(mol cm). Alternatively, the extinction coefficients of the drug and antibody in the HIC system were as follows: $\varepsilon_{\text{Ab},280} = 2.09 \times 10^5$ L/(mol cm), $\varepsilon_{\text{Ab},248} = 1.12 \times 10^5$ L/(mol cm), $\varepsilon_{\text{Drug},280} = 1.50 \times 10^3$ L/(mol cm), and $\varepsilon_{\text{Drug},248} = 1.59 \times 10^4$ L/(mol cm). The absorbance at each wavelength was associated with a specific retention time by setting the step size of data acquisition (0.2 s) rather than allowing automatic step size adjustment.

Reverse Phase Chromatography (RPC). Fraction collected samples from SEC runs were diluted to 1 mg/mL in Milli-Q deionized water and reduced with 50 mM DTT during a 30 min incubation at 37 °C. An Agilent 1200 series HPLC and a PLRP-S 5 um Varian column (50 × 2.1 mm, 1000 Å, 5 um) were used to separate each of the conjugated and unconjugated heavy and light chain species. Mobile phase A is composed of 0.1% TFA in Milli-Q deionized water, while mobile phase B is composed of 0.09% TFA in acetonitrile. A column temperature of 70 °C and a flow rate of 0.25 mL/min were used over the entire gradient in the following manner: 28.5% mobile phase B ranging from 0 to 3 min, 28.5−45.6% B from 3 to 60 min, 45.6−80% B from 60 to 61 min, 80% B from 61 to 64 min, 80−28.5% B from 64 to 65 min, and 28.5% B from 65 to 85 min. Thirty micrograms (30 μL) of each fraction collected sample were injected onto the column in duplicate. The original sample from which the fractions were obtained was also injected onto the column.

Differential Scanning Calorimetry (DSC). DSC analysis was performed using a VP Capillary DSC (MicroCal, Northampton, MA) calorimeter with a scan rate of 1 °C per minute over 60 min (25−90 °C). Data analysis was performed using Origin software (OriginLab, Northampton, MA). All samples were prepared for DSC by diluting them to 1 mg/mL in 20 mM buffer pH 5.5. The $T_{\text{m,onset}}$ is defined as the qualitative temperature at which the thermogram appears to have a nonzero slope. The T_m is defined as the temperature at which half of the molecules in a set are unfolded, and is calculated as the temperature value corresponding to each peak maximum on the thermogram.[16] The T_m value referenced in this paper, and that which is most relevant to ADC thermal stability, is the first T_m (corresponding to that of the CH_2 domain).[16]

Far UV Circular Dichroism. Far UV CD was performed using a Jasco J-815 Circular Dichroism Spectrometer (Jasco, Inc., Easton, MD) with an absorption range of 190 to 250 nm. Samples were diluted 25 fold in Milli-Q water to approximately 0.4 mg/mL, and 200 μL of the diluted sample were transferred to a Hellma (Plainview, NY) 0.5 mm cuvette. Cuvettes were thoroughly cleaned with water and methanol prior to the addition of each sample. All CD spectra were obtained using a continuous scanning method with a scan rate of 10 nm/min, data pitch of 1.0 nm, spectral bandwidth of 2.0 nm, data integration time of 8 s, and sample temperature of 22−24 °C (room temperature). Each sample spectra was collected as an average of four scans. The spectra for the ADC 1 research lots and unconjugated precursor, however, represent an average of 12 scans (4 scans/day for 3 days). The mean residue ellipticity was calculated using a residue number of 1326, a cuvette path length of 0.05 cm, and sample concentrations determined by UV spectroscopy.

CE-SDS. Samples were diluted to 1 mg/mL in labeling reaction buffer (0.1 M sodium Phosphate pH 6.7). Three hundred microliters of material were loaded onto NAP-5 Exchange columns (GE Healthcare) to buffer exchange them. The columns were washed with 400 μL of labeling buffer prior to elution with 500 μL of buffer. Buffer exchanged sample was combined in an 8:1 ratio with 2% SDS, 150 mM NEM (Fluka Analytical), and incubated at 70 °C for 5 min. After cooling, 10 μL of 2.5 mM 3-(2-furoyl)quinoline-2-carboxaldehyde (FQ Dye, Molecular Probes) were added to the sample, along with 10 μL of 30 mM KCN (Molecular Probes). The mixture was incubated at 50 °C for 10 min. The reaction was quenched by adding 700 μL of 1% SDS to each sample. Reduced samples were prepared by adding 10 μL of 1 M DTT to 200 μL of the quenched (nonreduced) samples, and incubating samples at 70 °C for 10 min. All samples were spun down at 1000 rpm for 2 min prior to analysis. CE-SDS analysis was performed using a Beckman PA 800 Plus. This method uses an uncoated 50 cm capillary (Beckman Coulter) placed 35 cm from the detector. The sample degradation products are separated electrophoretically for 35 min by a 15 kV voltage in reverse polarity (− to +). The capillary temperature was set to 40 °C.

Intrinsic Tryptophan Fluorescence. Fluorescence measurements were performed on a Jobin Yvon-Spex Fluoromax 2 fluorometer (Instruments S. A., Inc., Edison, NJ). All samples were excited at 295 nm, and the emission intensity was monitored for 0.1 s intervals at unitary wavelengths between 337 and 343 nm. Samples were diluted to 0.2 mg/mL in water

prior to analysis, and all scans were performed at room temperature. The ADC 1 research lots and unconjugated precursor were assayed a total of 12 times (4 scans/day for 3 days), and the sample error (±1 standard deviation) for the ADC 1 precursor and DAR 6 samples were calculated. *P*-values were used to determine the statistical significance of differences in fluorescence between samples.

RESULTS AND DISCUSSION

In this study, the effects of conjugation on the secondary and tertiary structures of an antibody conjugated to the vc-MMAE linker drug, as well as the physical stability of ADCs measured by changes in response to thermal stress, were explored. Far UV CD, intrinsic tryptophan fluorescence, and DSC were used to understand how the process of conjugation, which breaks the interchain disulfide bonds, affects antibody structure. The effect of thermal stress on the physical stability of an ADC was explored using ADC 1, which exhibits the rapid formation of high molecular weight species (HMWS) at 40 °C; this HMWS was characterized by SEC, SEC-MALS, DAR by UV absorbance, CE-SDS, far UV CD, DSC, and RPC. Furthermore, in order to discover any stability trends associated with increasing the average DAR, three lots of ADC 1 with different average DARs were placed on stability at 40 °C and analyzed by the aforementioned analytical methods. Lastly, we compared the biophysical stability of ADC 1 to seven other ADCs in an effort to learn more about the physical stabilities of this class of ADCs. Since all eight ADCs were conjugated in constant regions of the antibody, comparisons of these ADCs provided some insight on the effect of the variable domain on ADC biophysical stability.

Hydrophobic Interaction Chromatography (HIC). In order to determine the DAR distribution of ADC 1, and ultimately understand how drug load could affect the stability of an ADC, HIC was performed on an unstressed ADC 1 sample. Figure 2 shows the drug distribution profile of ADC 1, and the

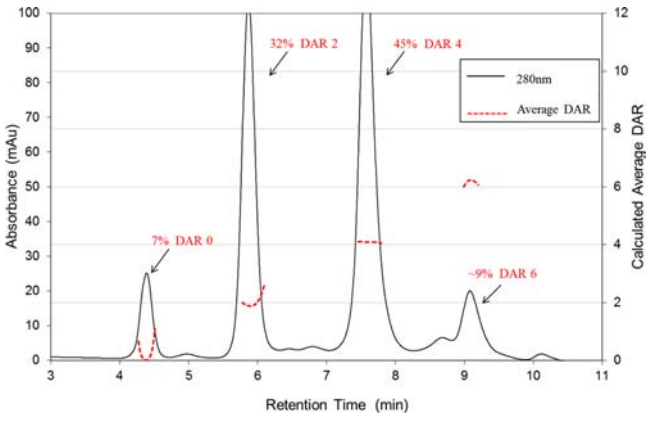

Figure 2. HIC chromatogram (280 nm) of an unstressed ADC 1 DAR 3.5 t0 sample with relative percentage areas and average calculated DAR of each major species.

relative percentages of each sub species of specific DARs. The average DAR of each peak was calculated using the UV absorbance at each peak maximum. Since the drug linker and protein have a maximum absorption at 248 and 280 nm, respectively, the total absorbance at each of the two wavelengths can be deconstructed into the sum of the absorbances of the drug and the antibody by applying Beer's law. The division of one equation by the other produces an expression that uses these total absorbances and the extinction coefficients of the drug and the antibody at the relevant wavelengths to calculate C_{drug}/C_{Ab}, or DAR, as illustrated by Hamblett et al (eq 2).[15] With the appropriate extinction coefficient, the equation can be used to understand how the drug distribution changes across the HIC chromatogram (for a single sample) and over time (for comparison of many stability samples). As is expected for an antibody with average DAR 3.5, ADC 1 contains mostly DAR 2 and DAR 4 species, with approximately 32% and 45% relative area being assigned to these species, respectively. Furthermore, the DAR 6 species accounts for approximately 9.2% of all species, while the DAR 8 species is not clearly detected by UV calculations. At this point, it is unclear how the DAR 8 species interacts with and elutes off of the column.

Effect of Conjugation on the Antibody Secondary and Tertiary Structure. Prior studies on ADCs confirm that the conjugation process itself does not affect the overall quaternary structure of the antibody, such that the ADC has an undiminished antigen binding capacity and minor linker-drug loss.[11,17] However, conjugation could potentially affect the secondary or tertiary structure of an antibody, since two or more largely hydrophobic drug residues are now present as part of the antibody structure on the heavy and/or light chains. In order to understand the effect of conjugation on the antibody secondary structure, far UV CD was performed on the unconjugated precursor of ADC 1, as well as on three lots of ADC 1 with average DAR 2, 3.5, and 6 to reveal differences in secondary structure upon conjugation, as described by Wankakar et al.[18] Figure 3 shows an average of 12 far UV

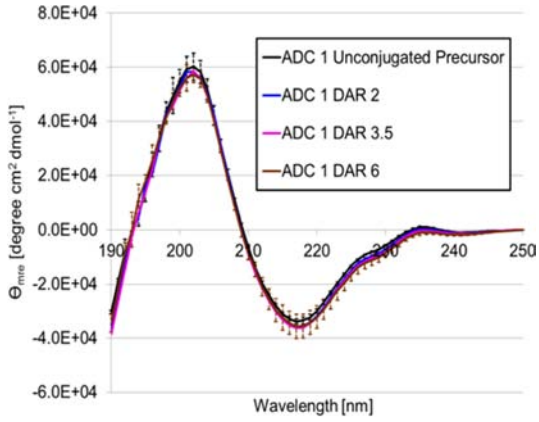

Figure 3. Far UV analysis of the t0 unconjugated ADC 1 precursor and t0 ADC 1 Lots of average DAR 2, 3.5, and 6. Each sample was run on three separate days in quadruplet. Each sample spectrum represents the average of 12 runs. For clarity, error bars (±1 standard deviation from the average) are only shown for the ADC 1 precursor and ADC 1 DAR 6 samples.

CD scans per sample. The error bars, which represent ±1 standard deviation from the average, are shown for only the ADC 1 unconjugated precursor and the ADC 1 DAR 6 sample. Based on this data and standard deviation spread between the two samples, it is concluded that the secondary structure is not measurably altered by conjugation.

The effect of conjugation on the tertiary structure of the antibody was investigated using both DSC and intrinsic tryptophan fluorescence. Near UV CD was not used because

dx.doi.org/10.1021/bc400182x | *Bioconjugate Chem.* 2013, 24, 1674−1683

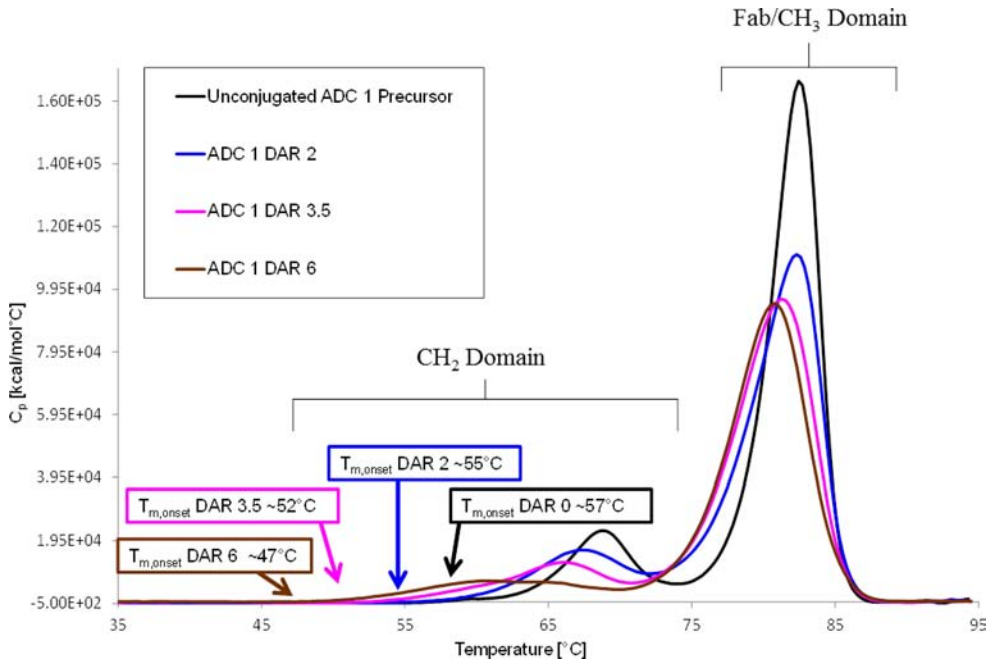

Figure 4. DSC thermograms of the unconjugated ADC 1 precursor andADC 1 Lots of average DAR2, 3.5, and 6.

the absorption spectra would include the strong absorbance of the drug moiety in the wavelength range of 240−260 nm (absorption maximum @ 248 nm). For typical IgG1 antibodies, DSC allows for the determination of the unfolding temperatures and unfolding temperature onsets of the CH_2, CH_3, and Fragment antigen-binding (Fab) domains of the antibody; consequently, changes in these values can signify changes in the response of the antibody's tertiary structure to thermal stress. For conjugates, it was anticipated that the CH_2 domain would be disproportionately impacted because of its proximity to the hinge region of the antibody, which contains 4 potential conjugation sites. DSC data on three lots of ADC 1 with varying average DARs shows that the melting temperature onset, or the qualitative temperature at which the thermogram appears to have a nonzero slope, of the CH_2 domain decreases as the average DAR increases (Figure 4); with respect to the unconjugated precursor, the melting temperatures of the DAR 2, DAR 3.5, and DAR 6 lots decrease by approximately 2 °C, 5 °C, and 10 °C, respectively. Additionally, the CH_2 domain of the DAR 6 material can be deconstructed into at least two species, with melting temperatures of approximately 60 and 64 °C. These two species could represent CH_2 domains with different drug loads in the hinge region, since an ADC with an average DAR of 6 will have a preponderance of CH_2 domains in which either two or four thiols in the hinge region are conjugated.[13] In contrast, the CH_3/Fab domains for the three lots of ADC 1 only decrease by a maximum of 2 °C after conjugation. More specifically, there is a slight trend in the peak shift with increasing DAR; the unconjugated precursor and the DAR 2 Fab/CH_3 domain peaks shift by a smaller amount than the DAR 3.5 and 6 peaks. It is unclear as of yet whether this trend is due to the possibility that the Fab domain is more likely to be conjugated, and subsequently destabilized, as the average DAR increases, or the possibility that the CH_3 domain is increasingly destabilized as conjugation in the hinge region becomes more prevalent. Nonetheless, it is clear that CH_3 or Fab domains are far less destabilized than the CH_2 domain upon conjugation.

In addition to DSC, the intrinsic fluorescence of a protein can provide useful information about the effect of conjugation on the tertiary structure of an ADC. Typically, the total intrinsic fluorescence is a mixture of the fluorescence from individual aromatic residues. The fluorescence emissions are partially due to the excitation of tryptophan residues, which are excited at 295 nm and fluoresce between 330 and 350 nm, depending on the local environment around these residues.[19] A shift in the peak maxima and/or a change in peak intensity is indicative of conformational changes at a given temperature.[19] Peak shifting, relative to the unconjugated precursor, was not evident in the spectra of DAR 2, DAR 3.5, and DAR 6 ADC 1 (SI Figure S2). Furthermore, while there appears to be a decrease in the intensity of DAR 6 species compared to others, the difference at peak maximum (λ = 335 nm) between the unconjugated precursor (peak with the highest intensity) and ADC 1 DAR 6 (peak with the lowest intensity) is not statistically significant (p = 0.14). Therefore, this data suggests that changes in the tryptophan microenvironments of ADC 1 are minimal or masked upon conjugation.

Overall, analysis of the three lots of ADC 1 revealed that conjugation does not measurably alter the antibody secondary or tertiary structures, but does render the tertiary structure more susceptible to unfolding when thermally stressed.

Characterization of ADC 1 HMWS. ADC 1 comprises chemically heterogeneous species that have different conjugation sites and drug loads, and may have different stabilities because of the structural modifications that occur during the conjugation process. DSC analysis revealed that conjugation impacts the response of the antibody tertiary structure to thermal stress. Therefore, we used a stress temperature of 40 °C to help elucidate thermal stability differences between the conjugated species of ADC 1. We specifically focus on the propensity of conjugates to aggregate, since aggregates can affect the immunogenicity and safety of the therapeutic.[20]

Size Exclusion Chromatography (SEC). In contrast to its unconjugated precursor, 40 °C incubation of ADC 1 results in the rapid formation of a HMWS comprising two peaks, eluting

dx.doi.org/10.1021/bc400182x | *Bioconjugate Chem.* 2013, 24, 1674−1683

at 11.7 and 13 min by SEC (Figure 5). The hydrodynamically larger HMWS (11.7 min peak) has an initial rate of formation

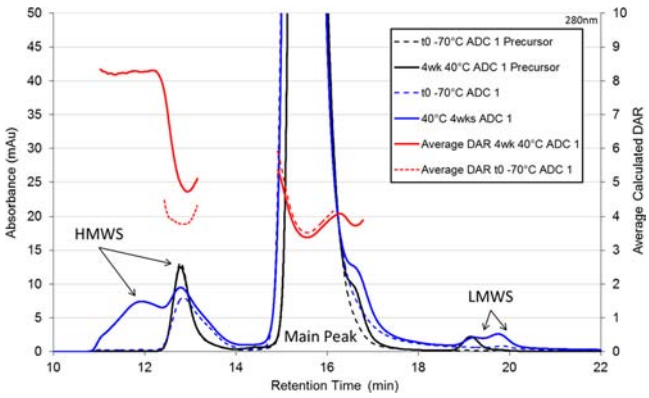

Figure 5. SEC chromatographs (λ = 280 nm) of t0 and 4 week 40 °C DAR 3.5 ADC 1 stability samples with average DAR calculations for the HMWS and main peak.

of approximately 0.2% per day, and grows to approximately 3.3% after 4 weeks at 40 °C. On the other hand, previous analysis of the unstressed (t0) 13 min HMWS peak by MS-MS revealed that it originally comprised covalently linked dimer species with an average DAR of 3.5 (data not shown). The growth of this peak on stability can be attributed either to spillover from the 11.7 min peak or to growth of a unique species. SEC with multiangle light scattering (MALS) detection showed that the larger (11.7 min) and smaller (13 min) HMWS comprise species with masses consistent with those of trimers and dimers, respectively (MALS data not shown). Furthermore, both ADC 1 HMWS are irreversibly formed, since SEC fraction-collected HMWS that was reformulated in the same buffer as the original sample at 1.5 mg/mL, and stored at 5 °C for over 3 weeks, did not dissociate into main peak upon reinjection onto the SEC column (data not shown). It is possible that the HMWS could be slowly reversed at temperatures and time points much greater than 3 weeks at 5 °C, but because the purification of this species, which, for a reversible process, would result in a major equilibrium shift, did not yield any increase in main peak, this HMWS is considered irreversible.[21]

In order to further characterize the HMWS of ADC 1, the average DAR of each peak on the SEC chromatogram was calculated using the UV absorbance at each peak maximum. Characterization of both ADC 1 HMWS peaks indicate that they have an average drug load range of 5−8 after 4 weeks at 40 °C (Figure 5). The 11.7 min HMWS peak has a DAR of approximately 8 ± 0.2, and the composition of this HMWS does not change after the first week of incubation; samples stressed from 1 to 8 weeks at 40 °C all result in a DAR value of 8 ± 0.2 (SI Figure S3). Therefore, this peak could contain a mixture of DAR 6 and DAR 8 species, since a peak with a composition of 20% DAR 6 species would still yield an average overall DAR of 7.8, which is still within the assay variability of the method (approximately 0.2 DAR). The smaller HMWS peak has a DAR of ∼5 after 4 weeks at 40 °C, and is likely the result of the combination of DAR 6 aggregate that forms on stability and the DAR 3.5 covalently bonded aggregate that was already present in the t0 sample. To confirm this observation, a different lot of ADC 1 with no 13 min peak at t0 was incubated for 4 weeks at 40 °C. DAR by UV analysis shows that the 13 min peak that forms on stability is a DAR 6 species (data not shown). By this method, the DAR 6 and DAR 8 species are the likely contributors of the HMWS formation, and can either be formed by an antibody conjugated to 6 or 8 drugs, or from fragments (with altered extinction coefficients) that have the appropriate ratio of absorbances at 248 an 280 nm to yield a calculated DAR of 6 or 8.

Reverse Phase Chromatography (RPC). To determine whether the HMWS species is composed of DAR 6 or DAR 8 species, fragments, or a combination of both, the 11.7 min HMWS and main peak fractions were collected off of the SEC column. The smaller 13 min HMWS peak was not fraction-collected or analyzed because the presence of disulfide-linked dimer in the t0 and stressed stability samples could confound results. All fraction collected samples were not turbid and contained no particulates visible to the human eye. Characterization of these samples by RPC under reducing conditions allowed for the elucidation of the distribution of drug-loaded heavy and light chains.

RPC under reducing conditions separates the heavy and light chains by hydrophobicity, such that the heavy chains with the highest drug load will have the latest elution time. For a given sample, one is able to determine the percentage of single- (HC + 1 vcMMAE), double- (HC + 2 vcMMAE), or triple- (HC + 3vcMMAE) conjugated heavy chain species in solution, in addition to the percentage of unconjugated species.[18] For light chain species, unconjugated and singly conjugated species are also resolved. Figure 6a shows the RPC chromatograms for the

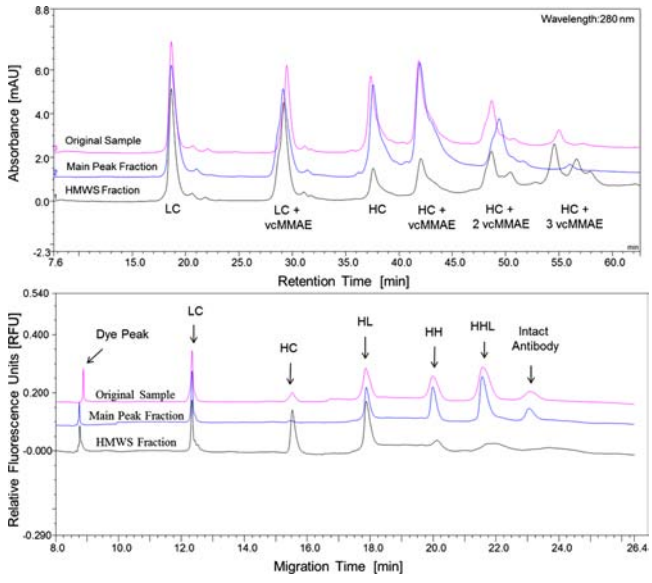

Figure 6. a. RP-HPLC chromatograms for the fraction collected ADC 1 main peak and HMWS species under reducing conditions. b. CE-SDS electropherograms of the HMWS fraction, main peak fractions, and the original 6 week 40 °C ADC 1 sample under nonreducing conditions. HC = heavy chain; LC = light chain; HL = heavy chain + light chain; HH = two heavy chains; HHL = 2 heavy chains + 1 light chain.

fraction collected SEC main peak and the HMWS species. A comparison of the main peak and the HMWS chromatograms shows that while the light chain content is similar among the two species, the heavy chain content is different. Particularly, the HMWS fraction contains a much higher proportion of a triply conjugated heavy chain species compared to the main

dx.doi.org/10.1021/bc400182x | Bioconjugate Chem. 2013, 24, 1674−1683

peak fraction; the main peak fraction contained approximately 5% triply conjugated heavy chain, while the HMWS fraction contained almost 45%. Alternatively, the HMWS fraction contained significantly less singly conjugated heavy chain compared to the main peak fraction (20% and 45%, respectively). Since the triple-conjugated HC is most likely to be involved in high DAR ADC species, this data confirms the hypothesis that the HMWS is has a larger proportion of higher DAR species than the monomer species.

Capillary Electrophoresis-Sodium Dodecyl Sulfate (CE-SDS). Similarly, nonreducing CE-SDS can also reveal useful information about extent and location of conjugation on heavy and light chain subunits. Under nonreducing conditions, the conjugated heavy and light chains of an antibody will dissociate to produce fragments of various sizes, depending on the number and location of disulfide bonds still present in the conjugated molecule. These fragments typically consist of heavy chain (HC), light chain (LC), heavy–light (HL), heavy–heavy–light (HHL), and the heavy–heavy–light–light (HHLL or intact antibody) species, as demonstrated by Wakankar et al.[18] Theoretically, a HMWS fraction mostly rich in only DAR 6 or DAR 8 species should produce an electropherogram consisting of mostly HC, LC, and HL, since there are no disulfide bonds holding the antibody quaternary structure together in a DAR 8 species, and the DAR 6 species has been shown to contain antibodies with mostly fully loaded hinge regions.[13] The electropherograms of the HMWS and main peak fractions of a 6 week 40 °C ADC 1 sample are shown in Figure 6b. The HMWS fraction shows the presence of mainly HC, LC, and HL residues. Furthermore, in comparison to the main peak fraction and the original 6 week 40 °C sample, the low signal of heavy–heavy fragments of all types indicates that HMWS heavy chains are mostly doubly conjugated in the hinge region, since the heavy chain–heavy chain interaction in SDS is dependent upon the presence of at least one disulfide bond. Furthermore, species of lower DAR (DAR 2, DAR 4) are not likely to produce such a distribution because of the increased likelihood of the presence of at least one unconjugated disulfide bond in the hinge region of the antibody,[13] as confirmed by the CE-SDS analysis of the unstressed DAR 2 and DAR 3.5 ADC 1 research lots (data not shown). Thus, the CE-SDS data supports the finding that the HMWS is mostly composed of DAR 6 and DAR 8 species, since the dissolution of these species in SDS would result in the strong presence of H, L, and HL residues, and ultimately the reduced presence of heavy–heavy fragments. The reverse phase and CE-SDS data both suggest that conjugation of both disulfide residues in the hinge region of the heavy chain contributes to the formation of the unstable high DAR species, which have a propensity to form noncovalently linked HMWS at stressed temperatures.

CE-SDS under reducing conditions was performed to determine whether the HMWS contained fragment, which in this study is defined as clipped or one-armed antibodies. In an intact antibody, the overall ratio of heavy chain to light chain should theoretically remain constant, regardless of DAR, once the antibody is reduced. Analysis of the 6 week 40 °C sample, its HMWS fraction, and main peak fraction by reduced CE-SDS show that all three samples contain the same ratio of heavy chain to light chain (65%:35%) (electropherogram not shown). Therefore, the HMWS does not contain any fragment, to a measurable extent, because the presence of fragment would either alter the ratio of heavy chain to light chain and/or generate new peaks on the electropherogram. It is also worth noting that HC or HL residues from a DAR 6 or DAR 8 antibody could theoretically dissociate from the antibody under stress and aggregate; in other words, the aggregate could be formed from a random mix of aggregated and drug-loaded HC, HL, and LC residues. However, this scenario seems implausible given that two peaks of DAR 6 and DAR 8 were resolved by SEC, and a random mix of drug loaded HC, HL, and LC would not yield such specific DAR values. As a result, the existing data indicates that the HMWS formed by ADC 1 largely comprises intact aggregated DAR 6 and DAR 8 species.

Far UV CD and DSC. To further assess whether the HMWS involves a structurally altered or native form of ADC 1, far UV CD and DSC studies were performed on the fraction collected HMWS and main peak (from SEC). Far UV CD data (Figure 7a) shows that the HMWS has a different secondary structure

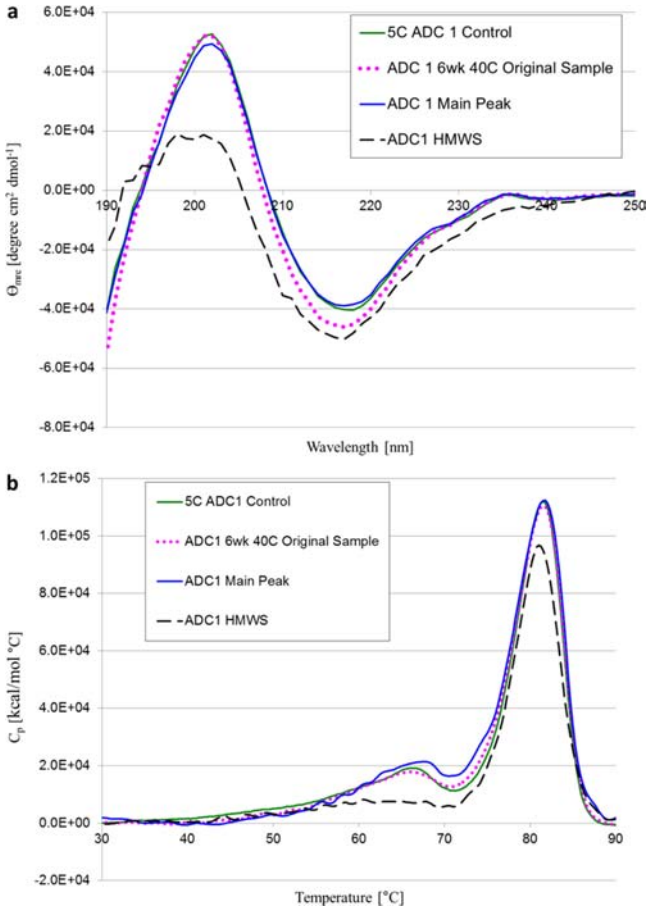

Figure 7. Far UV CD (a) and DSC thermogram (b) of the fraction collected HMWS, fraction collected main peak, 6 week 40 °C original sample, and 5 °C control.

compared to the main peak fraction; more specifically, the former fraction likely contains a higher percentage of β-sheets, which yield a more intense minimum at 217 nm. This data suggests that while the conjugation of high DAR species does not itself result in major changes in the protein backbone as shown by Figure 2, the secondary structures of the high DAR species are in fact altered by the addition of thermal stress post conjugation.

Furthermore, since the ADC forms aggregates rather readily at 40 °C compared to the unconjugated precursor, and the unfolding temperature of the CH_2 domain is lowered for the

dx.doi.org/10.1021/bc400182x | *Bioconjugate Chem.* 2013, 24, 1674–1683

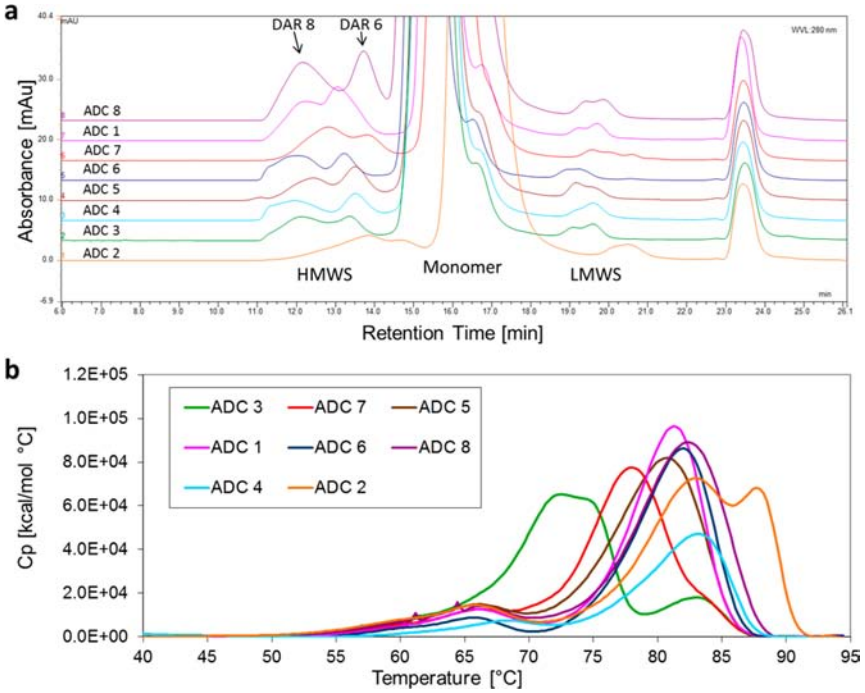

Figure 8. a. SEC chromatograms (λ = 280 nm) of 4 week 40 °C samples from ADC 1 to 8 The 11.7 and 13 min HMWS peaks were found to have an approximate DAR of 6 and 8 (by DAR by UV), respectively, for all ADCs except for ADC 1 (DAR of 5), which contained a significant amount of DAR 3.5 13 min HMWS in its t0 sample. b. Differential Scanning Calorimetry (DSC) thermograms of all eight ADCs.

ADC, we hypothesized that the CH_2 domain is implicated in the formation of aggregates for the ADC. To test this hypothesis, we subjected the HMWS fraction to DSC studies. As shown in Figure 7b, a much weaker unfolding transition, as indicated by the reduced height and area of the peak corresponding to the unfolding of the CH_2 domain, is observed for the CH_2 domain in the HMWS sample compared to the ADC main peak fraction (from SEC) or the ADC 5 °C control sample. This difference of approximately 1×10^4 kcal/mol °C in peak height is not due to differences in sample concentration, and suggests that a large proportion of CH_2 domains in the sample have already unfolded prior to sample analysis, since the mass of sample analyzed was the same for all samples. In other words, the CH_2 domain is already partially unfolded in the aggregate, and its instability prior to unfolding is likely the main cause of the formation of HMWS for ADC 1. Furthermore, the peak height of the Fab/CH_3 domain of the HMWS sample is also slightly lower, indicating that one of these regions in a small proportion of antibodies has also unfolded, although to a lesser extent than the CH_2 domain, prior to sample analysis. Overall, the data characterizing the HMWS suggests that a major contributor to aggregate formation in ADC 1 is the destabilization of the hinge region/CH_2 domain upon thermal stress caused by the presence of 4 linker drugs.

Effect of Average DAR on the Thermal Stability of ADC 1. ADC 1 aggregation data under stressed temperature conditions suggests that higher DAR species are responsible for the formation of HMWS at 40 °C. It would follow that ADC lots with higher average DARs would be more sensitive to thermal stress, as suggested by the trend in $T_{m,onset}$ values seen in Figure 3. Three research lots of ADC 1 with average DARs of 2, 3.5, and 6 were stressed at 40 °C in order to confirm the effect of average DAR on thermal stability.

Incubation of the different DAR lots at a stress temperature of 40 °C for up to 8 weeks shows that the initial rate of HMWS formation increases with increasing DAR (SI Figure S4a). ADC 1 lots of average DAR 2 and 3.5 appear to have a much lower rate of HMWS formation than the DAR 6 lot; the latter lot formed over 27% aggregate after 8 weeks, while the former two lots formed only 2−5% in the same time frame. Furthermore, reverse phase analysis of ADC 1 lots confirms that fraction collected HMWS from 4 week 40 °C samples have triple-conjugated heavy chain proportions that increase with average drug load (SI Figure S4b). All of the data on the various DAR lots correlate a higher DAR to decreased thermal stability, and subsequently the increased formation of a HMWS resulting from the increased percentage of DAR 6 and 8 species.

HMWS Formation in Other ADCs. Since HMWS formation at 40 °C in an ADC is due to the increased sensitivity of the tertiary structure to thermal stress, presumably due to the presence of conjugated drugs at the interchain cysteines close to the CH_2 domain, any ADC conjugated in the same fashion as ADC 1 is expected to produce a HMWS at 40 °C. Furthermore, this HMWS should consist of mainly higher DAR species. Eight ADCs (including ADC 1) with over 90% sequence homology (variability in the Complementarity determining regions/Fragment variable domain) were incubated for 4 weeks at 40 °C, and were analyzed by SEC in order to confirm that the resultant HMWS composition was not unique to ADC 1. All ADCs were manufactured with an average DAR of 3.5 in the same formulation, except for ADC 4 and ADC 8, which are formulated at 20 mM in different buffers at pH 6.5 and 6.0, respectively.

SEC chromatograms of these samples show that all eight ADCs form the larger HMWS comprised of DAR 6 and DAR 8 subspecies on stability (based on DAR by UV), with the latter species typically eluting before the former (Figure 8a). Furthermore, after 4 weeks at 40 °C, the percentage of HMWS generated over this time frame in each ADC ranges from 1.5% to 3.3% (relative percentage area), while the same

dx.doi.org/10.1021/bc400182x | Bioconjugate Chem. 2013, 24, 1674−1683

percentage in the unconjugated ADC precursors ranges from 0% to 0.3%. This data is interesting given that all of the antibodies are conjugated in the constant regions of the protein subunits, and would thus be expected to form the same amount of high DAR HMWS over a 4 week period at 40 °C. The differences in the absolute percentages of HMWS were not due to differences in the relative percentages of each DAR species in the t0 samples, as HIC chromatograms of the ADCs revealed similar DAR distributions (data not shown). Furthermore, DSC was performed to see if differences in the monthly rates of formation of HMWS might be due to differences in the stability of the CH_2 domain. The T_m and $T_{m,onset}$ values of the CH_2 domains are expected to be the most relevant to the instability of ADCs at higher temperatures, since a lower T_m or $T_{m\ onset}$ could translate to larger amounts of aggregate at these temperatures. For the most part, the ADCs have $T_{m,onset}$ values ranging from 50 to 54 °C, and all share the same T_m value, with the exception of ADC 4, which has a slightly larger T_m (Figure 8b). Additionally, even though ADCs 2 and 3 have Fab melting transitions that are lower and higher than their CH_3 domains, respectively, these ADCs still have distinct CH_2 melting transitions and onsets that overlap with the other six ADCs. Overall, the $T_{m,onset}$ values of all of the ADCs were not different enough to see any trends that correlate with the monthly rate of HMWS formation. We hypothesize that the differences in the monthly aggregation rates could be due to differences in the molecular properties of monoclonal antibodies, such as the variable domain sequence,[16] charge, overall hydrophobicity, structural dynamics, as well as the formation of other products such as deamidated species at 40 °C. Future studies will be conducted to further investigate this phenomenon.

CONCLUSIONS

The data presented in this paper reveal that conjugation of an antibody via the interchain disulfide bonds results in an ADC distribution in which the species with a fully drug-loaded hinge region (mainly DAR 6 and DAR 8) are relatively more unstable at stressed temperatures of 40 °C, compared to the low DAR/unconjugated species. More specifically, we show that conjugation involving the hinge disulfides, mostly in the DAR 6 and 8 species, affects the CH_2 domain thermal stability such that it unfolds at lower temperatures compared to that in the unconjugated precursor. Such instability manifests in the formation of aggregates (HMWS) at a relatively faster rate at 40 °C. It is important to note that while these ADCs do not experience rapid aggregate formation at the relevant storage temperature of 5 °C, the conjugation-induced instability in the CH_2 domain of high DAR species could manifest itself in other degradation pathways when the antibody is subject to other forms of stress (such as agitation, light exposure, oxidative stress, and dilution into IV bags) during manufacture.[21] Clearly, reducing the percentage of higher DAR species could decrease the sensitivity of ADCs to aggregation at elevated temperatures, and potentially other forms of physical degradation caused by CH_2 domain instability.

Interestingly, the variable regions and/or other properties of the ADCs may contribute to the formation of aggregate, since eight different ADCs conjugated in the constant regions of the heavy and light chain subunits exhibit monthly rates of HMWS formation that differ by up to a factor of 2. Elucidation of the factors that influence rates of HMWS formation in ADCs could potentially improve the early molecular assessment of ADC candidates with the same target, since those with poorer thermal stability could be eliminated. The careful selection of these ADC candidates can significantly reduce the effort that pharmaceutical scientists exert to create a stable antibody that is resistant to many forms of stress, and eventually save biopharmaceutical companies a substantial amount of investment.

ASSOCIATED CONTENT

Supporting Information

Figure S1: Drug load distributions of ADC 1 Lots of average DAR 2, 3.5, and 6 by HIC. Figure S2: Intrinsic Tryptophan Fluorescence of ADC 1 precursor and Conjugate Lots of average DAR 2, 3.5, and 6. Figure S3: SEC Chromatographs and DAR calculations for t0 through 8 week 40 °C ADC 1 Stability samples. Figure S4a: SEC Chromatograms and Kinetics of HMWS formation for 4 week 40 °C ADC Lots of average DAR 2, 3.5, and 6. Figure S4b: RP-HPLC of fraction collected HMWS from 4 week 40 °C ADC 1 lots. This material is available free of charge via the Internet at http://pubs.acs.org.

AUTHOR INFORMATION

Corresponding Authors

*Telephone: 650-467-2837; Fax 650-225-3613; E-mail: beckley.nia@gene.com.

*Telephone: 650-225-5758; Fax 650-225-3613; E-mail: flores.heather@gene.com.

Notes

The authors declare no competing financial interest.

ACKNOWLEDGMENTS

The authors want to thank Charity Betchel and Mary Nguyen for SEC-MALs analysis, John Briggs for the reverse phase assay and discussion, Tom Patapoff for the helpful discussion, and the ADC formulators (Lan Le, Bill Galush, Brian Connolly, Isabella de Jong, Erika Ingham, Pervina Kei, Yilma Adem, and Daren Nelson) for samples, data, and discussion.

ABBREVIATIONS

ADC, antibody–drug conjugate; CD, circular dichroism; DAR, drug-to-antibody ratio; DSC, differential scanning calorimetry; Fab, Fragment antigen-binding; HIC, hydrophobic interaction chromatography; HMWS, high molecular weight species; MALS, multiangle light scattering; RPC, reverse phase chromatography; SEC, size exclusion chromatography; vc-MMAE, val-cit-Monomethyl Auristatin E

REFERENCES

(1) Zhang, Q., Chen, G., Liu, X., and Qian, Q. (2007) Review Monoclonal antibodies as therapeutic agents in oncology and antibody gene therapy. *Cell Res. 17*, 89–99.

(2) Feld, J., Barta, S. K., Schinke, C., Braunschweig, I., Zhou, Y., and Verma, A. K. (2013) Linked-in: design and efficacy of antibody drug conjugates in oncology. *Oncotargets Ther. 4*, 397–412.

(3) Slamon, D. J., Leyland-Jones, B., Shak, S., Fuchs, H., Paton, V., Bajamonde, A., Fleming, T., Eiermann, W., Wolter, J., Pegram, M., Baselga, J., and Norton, L. (2001) Use of chemotherapy plus a monoclonal ADC against HER2 for metastatic breast cancer that overexpresses HER2. *N. Engl. J. Med. 344*, 783–792.

(4) Kemshead, J. T., and Hopkins, K. (1993) Uses and limitations of monoclonal antibodies (MoAbs) in the treatment of malignant disease: a review. *J. R. Soc. Med. 86*, 219–224.

(5) Singh, R., and Erickson, H. K. (2009) Antibody-cytotoxic agent conjugates: preparation and characterization. *Methods Mol. Biol. (N. Y., NY, U. S.) 525*, 445–467.

(6) Ritter, A. (2012) Antibody-drug conjugates: looking ahead to an emerging class of biotherapeutics. *Pharm. Technol. 36*, 42−47.
(7) Erickson, H. K., Park, P. U., Widdison, W. C., Kovtun, Y. V., Garrett, L. M., Hoffman, K., Lutz, R. J., Goldmacher, V. S., and Blattler, W. A. (2006) Antibody−maytansinoid conjugates are activated in targeted cancer cells by lysosomal degradation and linker-dependent intracellular processing. *Cancer Res. 66*, 4426−4433.
(8) Kung Sutherland, M. S., Sanderson, R. J., Gordon, K. A., Andreyka, J., Cerveny, C. G., Yu, C., Lewis, T. S., Meyer, D. L., Zabinski, R. F., Dorolina, S. O., Senter, P. D., Law, C. L., and Wahl, A. F. (2006) Lysosomal trafficking and cysteine protease metabolism confer target-specific cytotoxicity by peptide-linked anti-CD30−auristatin conjugates. *J. Biol. Chem. 281*, 10540−10547.
(9) Doronina, S. O., Mendelsohn, B. A., Bovee, T. D., Cerveny, C. G., Meyer, D. L., Oflazoglu, E., Toki, B. E., Sanderson, R. J., Zabinski, R. F., Wahl, A. F., and Senter, P. D. (2006) Enhanced activity of monomethylauristatin F through monoclonal antibody delivery: effects of linker technology on efficacy and toxicity. *Bioconjugate Chem. 17*, 114−124.
(10) Hamann, P. R., Hinman, L. M., Beyer, C. F., Lindh, D., Upeslacis, J., Flowers, D. A., and Bernstein, I. (2002) An anti-CD33 antibody−calicheamicin conjugate for treatment of acute myeloid leukemia. Choice of linker. *Bioconjugate Chem. 13*, 40−46.
(11) Junutula, J. R., Raab, H., Clark, S., Bhakta, S., Leipold, D. D., Weir, S., Chen, Y., Simpson, M., Tsai, S. P., Dennis, M. S., Lu, Y., Meng, Y. G., Ng, C., Yang, J., Lee, C. C., Duenas, E., Gorrell, J., Katta, V., Kim, A., McDorman, K., Flagella, K., Venook, R., Ross, S., Spencer, S. D., Wong, W. L., Lowman, H. B., Vandlen, R., Sliwkowski, M. X., Scheller, R. H., Polakis, P., and Mallet, W. (2008) Site-specific conjugation of a cytotoxic drug to an antibody improves the therapeutic index. *Nat. Biotechnol. 26*, 925−32.
(12) Food and Drug Administration. (2013) FDA approves new treatment for late-stage breast cancer. [Press release]. Retrieved from http://www.fda.gov/NewsEvents/Newsroom/PressAnnouncements/ucm340704.htm.
(13) Le, L. N., Moore, J. M. R., Ouyang, J., Chen, X., Nguyen, M. D. H., and Galush, W. J. (2012) Profiling antibody drug conjugate positional isomers: a system-of-equations approach. *Anal. Chem. 84*, 7479−7486.
(14) Seegan, G. W., Smith, C. A., and Schumaker, V. N. (1979) Changes in quaternary structure of IgG upon reduction of the inter heavy-chain disulfide bond. *Proc. Natl. Acad. Sci. U.S.A. 76*, 907−911.
(15) Hamblett, K. J., Senter, P. D., Chace, D. F., Sun, M. M. C., Lenox, J., Cerveny, C. G., Kissler, K. M., Bernhardt, S. X., Kopcha, A. K., Zabinski, R. F., Meyer, D. L., and Francisco, J. A. (2004) Effects of drug loading on the antitumor activity of a monoclonal antibody drug conjugate. *Clin. Cancer Res. 10*, 7063−7070.
(16) Ionescu, R. M., Vlasak, J., Price, C., and Kirchmeier, M. (2008) Contribution of variable domains to the stability of humanized IgG1 monoclonal antibodies. *J. Pharm. Sci. 97*, 1414−1426.
(17) Francisco, J. A., Cerveny, C. G., Meyer, D. L., Mixan, B. J., Klussman, K., Chace, D. F., Rejniak, S. X., Gordon, K. A., DeBlanc, R., Toki, B. E., Law, C. L., Doronina, S. O., Siegall, C. B., Senter, P. D., and Wahl, A. F. (2003) cAC10-vcMMAE, an anti-CD30-monomethyl auristatin E conjugate with potent and selective antitumor activity. *Blood 102*, 1458−1465.
(18) Wakankar, A., Chen, Y., Gokarn, Y., and Jacobson, F. S. (2011) Analytical methods for physicochemical characterization of antibody drug conjugates. *MAbs 3*, 161−172.
(19) Vivian, J. T., and Callis, P. R. (2001) Mechanisms of tryptophan fluorescence shifts in proteins. *Biophys. J. 80*, 2093−3109.
(20) Hermeling, S., Crommelin, D. J., Schellekens, H., and Jiskoot, W. (2004) Structure-immunogenicity relationships of therapeutic proteins. *Pharm. Res. 21*, 897−903.
(21) Cromwell, M. E. M., Hilario, E., and Jacobson, F. (2006) Protein aggregation and bioprocessing. *AAPS J. 8*, E572−E579.